Linear stability analysis of a High Performance Light Water Reactor.

Maarten in't Veld, June 2011

PNR-131-2011-008

Nomenclature

Roman letters

A	Cross-sectional area coolant	m^2
A_s	surface area of fuel rod	m^2
$C_{p,fuel}$	Specific heat of fuel	$J*kg^{-1}*K^{-1}$
D_H	Hydraulic Diameter	m
f	Darcy-Weisbach friction factor	-
g	Gravitational acceleration	$m*s^{-2}$
G	Mass flow	$kg*m^{-1}*s^{-2}$
h	Enthalpy	$J*kg^{-1}$
K	Local pressure drop coefficient	-
l	Lifetime of prompt neutrons	s
n_{out}	number of the node at the top of the fuel rod	
n_{in}	number of the node at the begin of the fuel rod	
p	Pressure	Pa
P	Heated perimeter	m
q''	Heat flux	$W*m^{-2}$
R_f	Radius of the fuel rod	m
t	Time	s
T_c	Cladding temperature	°C
T_{fuel}	Fuel temperature	°C
T_{Bulk}	Bulk temperature	°C
V_{fuel}	Volume of the fuel	m^3
v_n	Neutron velocity	$m*s^{-1}$
w_f	energy released per fission event	J/event
z	Spatial coordinate	m

Greek letters

α	coolant density	$kg*m^{-3}$
β_k	Delayed neutrons fraction	-
λ_k	decay constants of delayed neutrons	s^{-1}
λ_{th}	thermal conductivity	$Wm^{-2}K^{-1}$
ϑ	Angle between flow and horizontal	rad.
ρ	Density	$kg*m^{-3}$
$\tilde{\rho}$	Average coolant density	$kg*m^{-3}$
$\rho_{reactivity}$	Reactivity	
Λ_{gen}	mean neutron generation time	s
μ	dynamic viscosity	Pa s
$\sum$	macroscopic cross-section of fission event	m^{-1}
τ	Time delay	s

Content

1. Introduction

The HPLWR (High Performance Light Water Reactor) is a generation IV nuclear reactor design that is being developed as part of the international generation IV forum (GIF)[i]. The goal of the GIF is the development of new nuclear reactor technologies that meet certain demands. These demands are formulated in eight goals concerning "*Sustainability*", "*Economics*", "*Safety and Reliability*" and *"Proliferation Resistance and Physical Protection*". As such these reactors must be safer, provide a better proliferation resistance and of course a higher thermal efficiency.
For this development six promising technologies were chosen:
the Gas-Cooled Fast Reactor (GFR)
the Sodium-Cooled Fast Reactor (SFR)
the Lead-Cooled Fast Reactor (LFR)
the Very High Temperature Reactor (VHTR)
the Molten Salt Reactor (MSR)
the Supercritical Water Reactor (SCWR).

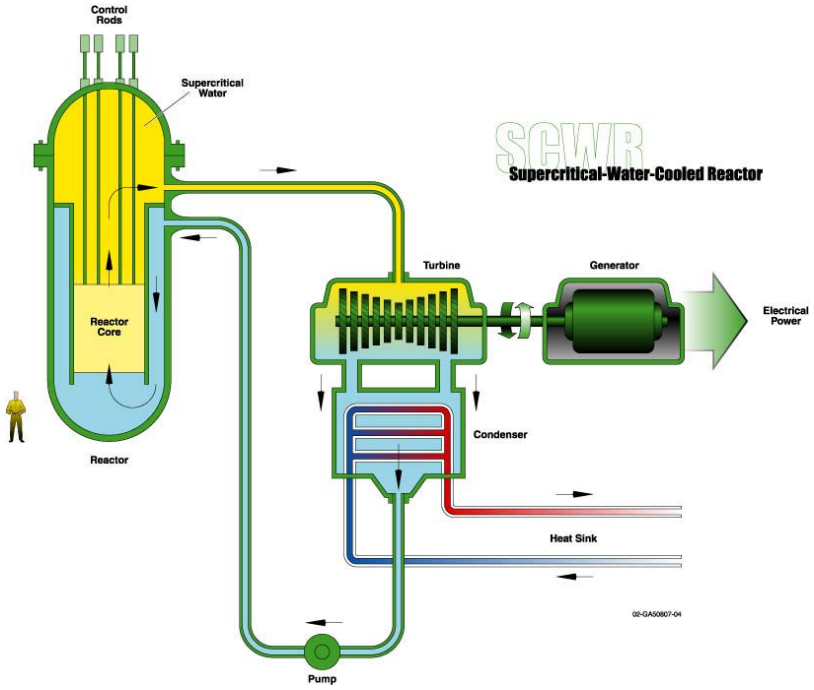

Figure 1.1: Simplified model of SCWR

The HPLWR is a specific type of a SCWR, Figure 1.1: Simplified model of SCWR shows a simplified representation of a SCWR. On the left there is the reactor core in which "cold" water of about 280°C flows into the Reactor Pressure Vessel. In the core the water is heated up to 500°C.
After passing through the core, the water flows through the turbine, transferring energy to drive a generator which produces the electricity. What remains in excess heat is removed in the condenser. It is important to note that the water does not change phase, there is no boiling. This is different from nuclear reactors today. This is because the pressure is above the critical pressure, the water is thus supercritical.

The HPLWR operates at a pressure of 25 MPA. At this pressure the water will be supercritical, if the temperature is above 373.9°C (Figure 1.2Figure 1.2 phase changes fluid figure is adopted from Gomez(2009)).

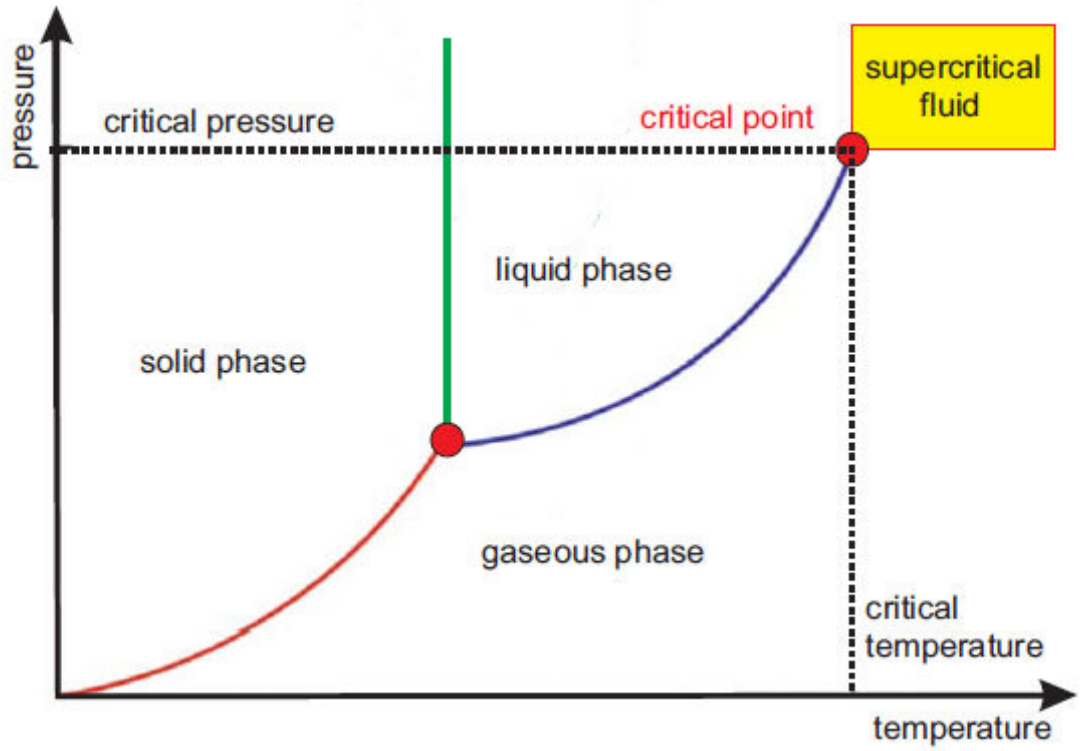

Figure 1.2 phase changes fluid figure is adopted from Gomez(2009)[viii]

A unique feature of the HPLWR is the fact that it has a three-pass-core. In order to prevent to high local cladding temperatures, the water is heated up in three stages, in between which the water is mixed in order to achieve a more homogeneous temperature. In Figure 1.3 the flow of the water through the core is schematically depicted. In the RPV there is a total of 156 Fuel Assembly Clusters (FAC) (Figure 1.4), the three core sections (evaporator and the two super heaters) each have 52 FAC's.

In a fuel assembly the water flow between the fuel rods (yellow in Figure 1.3) is upwards, the water acts as a coolant here, in the middle is the moderator box where the water flows downwards and acts as a moderator.

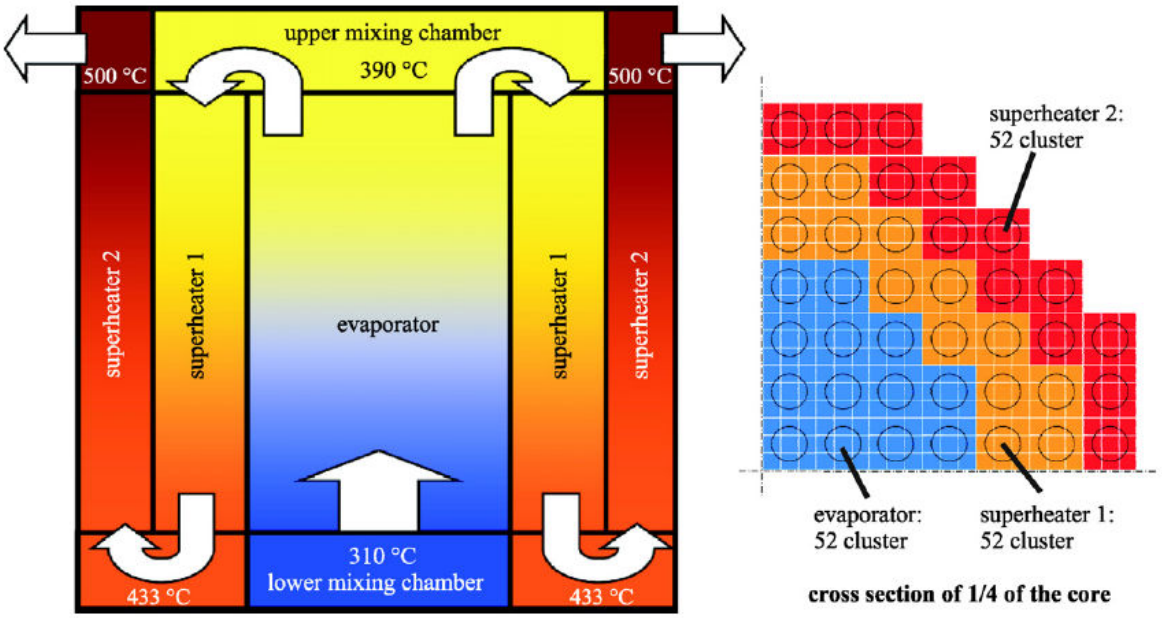

Figure 1.3: Schematic three pass core of a HPLWR, figure adopted from Fischer et al (2009)

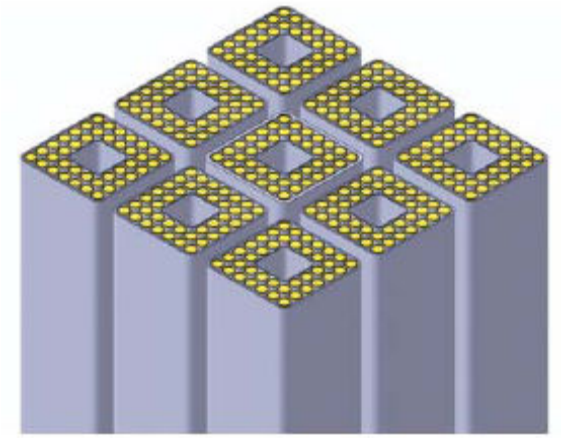

Figure 1.4: one fuel assembly cluster, one cluster consists of 9 fuel assemblies, 1 fuel assembly consists of 40 fuel rods. The fuel flows as a moderator through the centre, while it flows as a coolant between the fuel rods. Figure adopted from Gomez (2009)[viii]

Water as a moderator

The heat production in a HPLWR is driven by nuclear fission, which in turn is controlled by the moderating effect of the water.

The nuclear fission is induced by the neutrons released in previous fissions. The neutrons however have to be slowed down to make a new collision possible, as this is a thermal reactor.

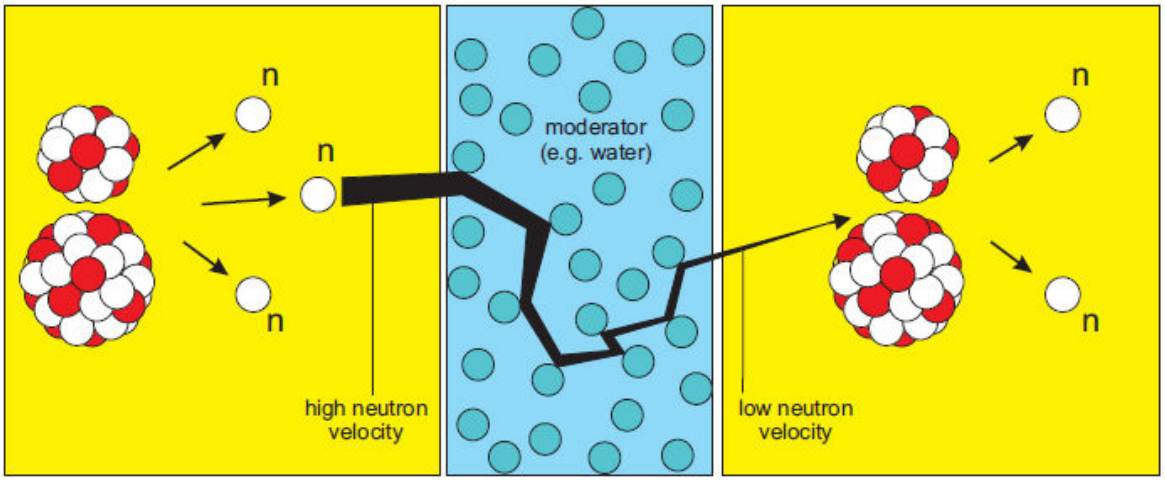

Figure 1.5: fission in nuclear chain reaction, figure is adopted from Gomez (2009)viii

If there is an increase of heat production in the core, the density gets lower, reducing the moderating effect of the water, so the number of fissions will reduce which will reduce the heat production. This is a stabilising negative feedback.

Stability

Nuclear reactors are complex systems containing multiple feedback mechanisms. These mechanisms interact and can cause the system to become unstable. A system is considered to be in a stable state if once perturbed from that state, it will return to its original state .The system is deemed unstable if perturbation results in an excursion to another state (static instability) or into growing oscillations (dynamic instabilities). Because of changes in density ,mass-flow rate and the power coupling, the studied system can become unstable

In this thesis the development (from an initial state) of the mass-flow, density and enthalpy of the coolant/moderator are being calculated, and are coupled with the neutron density and the power of the nuclear reaction. The stability of this coupled system is then analysed.

Model

There are two important types of oscillations, the in-phase “Density Wave Oscillation” and the out of-phase oscillation, see also chapter 3. At the in-phase an entire unstable region acts as one channel, this is the case that will be studied in this thesis.

All fuel assemblies clusters in a superheater or the evaporator have the same pressure difference, the mass flow can change per fuel assembly cluster but in this thesis only the case where the mass flow is the same for each fuel assembly cluster is considered. Because the pressure and the mass

flow are assumed to be the same for all fuel assembly clusters a model that considers a single fuel assembly cluster is proposed.
The boundary conditions that are considered here are the pressure at the inlet and at the outlet of the channel, the enthalpy of the water at the inlet, the friction at the inlet, the friction at the outlet and the friction in the channel.

Outline

A model simulating the flow in a thermo-hydraulic system with constant power production has been developed by G. Koren[vi]. The goal of this thesis is to implement nuclear fission as a power source by coupling the power production with the density field through the neutronic equations. In chapter 2 the required equations are derived, where the point kinetics model is used to describe the nuclear fission and the moderating influence of the water. In chapter 3 the instability mechanisms described and the method of analysing the point at which a system becomes unstable.
In chapter 4, the results are discussed and compared to the results of the original code where no nuclear fission was taken into account.

2. Equations

Initial equations

The equations consist of the original thermodynamics equations used by G. Koren[vi], and in addition the point kinetic model is used. There are three balance equations describing the conservation of mass, momentum and energy.

The point kinetic model (Duderstadt & Hamilton[ii]) is used to couple the power through the neutron density to the density of the moderator (by the reactivity feedback), Gomez[viii] also used this model to implement nuclear fission in the model. The equation that is used to calculate the reactivity feedback was proposed by Schlagenhaufer[iv].

The equations are based upon a one-dimensional model, with a constant cross-sectional flow area. The equations are immediately discretised using the following rules.

- All the variables that depend on z (space) are being discretised with an index i corresponding to a position (z).

$$y \rightarrow y_i \tag{1.1}$$

- Derivatives with respect to z (space) are being discretised as follows

$$\frac{\partial y}{\partial z} \rightarrow \frac{y_i - y_{i-1}}{\Delta z} \tag{1.2}$$

- Partial derivatives with respect to time (t) become regular derivatives

$$\frac{\partial y_i}{\partial t} = \frac{dy_i}{dt} \tag{1.3}$$

Balance equations

Mass equation:

$$\frac{\partial \alpha}{\partial t} + \frac{\partial G}{\partial z} = 0 \tag{1.4}$$

Discretisation

$$\frac{d\alpha_i}{dt} + \frac{G_i - G_{i-1}}{\Delta z} = 0 \tag{1.5}$$

Momentum equation:

$$\frac{\partial G}{\partial t}+\frac{\partial}{\partial z}\left(\frac{G^2}{\alpha}\right)+\frac{\partial p}{\partial z}=-g\sin(\theta)-\frac{1}{2}\frac{G^2}{\alpha}\left[\frac{f}{D_H}+\sum_j K_j\delta\left(z-z_j\right)\right] \quad (1.6)$$

Discretisation

$$\frac{dG_i}{dt}+\frac{1}{\Delta z}\left(\frac{G_i^2}{\alpha_i}-\frac{G_{i-1}^2}{\alpha_{i-1}}\right)+\frac{p_i-p_{i-1}}{\Delta z}=-g\alpha_i\sin(\theta_i)-\frac{1}{2}\frac{G_i^2}{\alpha_i}\left[\frac{f_i}{D_H}+\frac{K_i}{\Delta z}\right] \quad (1.7)$$

Energy equation:

$$\frac{\partial \alpha h}{\partial t}+\frac{\partial Gh}{\partial z}=q''\frac{P}{A} \quad (1.8)$$

Discretisation

$$\frac{d\alpha_i h_i}{dt}+\frac{G_i h_i-G_{i-1}h_{i-1}}{\Delta z}=q''_i\frac{P}{A} \quad (1.9)$$

Point Kinetics

Point kinetics (Duderstad & Hamilton) [ii] is the model that estimates the total power produced by the core, dependent on the number of fission events. The power increases with the number of fission events.

The number of fission events is dependent on the neutron population because of the production of both prompt and delayed neutrons. These latter are produced by the fission products and can have a time delay in the order of several milliseconds to a few seconds.

fractions	Decay constants
B_1=0.038	λ_1=0.0127 s^{-1}
B_2=0.213	λ_2=0.0317 s^{-1}
B_3=0.188	λ_3=0.0115 s^{-1}
B_4=0.407	λ_4=0.0311 s^{-1}
B_5=0.128	λ_5=1.4 s^{-1}
B_6=0.026	λ_5=3.87 s^{-1}

Table 2.1 parameters point kinetic model

In the point kinetic model the core is being seen as a whole i.e. there is no discretisation, this means that the number of variables to describe the system only increases with an extra eight: the neutron

density, the power and the six neutronic precursor concentrations, so the calculation time shouldn't increase much.
The density used in the neutronic calculation is the average density. Later in this chapter the possibility will be discussed to add a spatial dependence but in this study that option is not used.

w_f	$2.81 \cdot 10^{-11}$ J/per event		Σf	1.08456 m^{-1}
v_n	5729.58 m s^{-1}		*cp,*fuel	$0.116 \cdot 10^{3}$ J kg^{-1} K^{-1}
P_{fuel}	$10.96 \cdot 103$ kg m^{-3}		*V*fuel per rod	0.000148 m^3
A_s per rod	0.1055 m^2		*r*fuel	$3.35 \cdot 10^{-3}$ m
t_c	$0.5 \cdot 10^{-3}$ m		*tg*	$0.15 \cdot 10^{-3}$ m
k_f	25.9 W m^{-1} K^{-1}		*hg*	0.78 W m^{-1} K^{-1}
k_c	21.5 W m^{-1} K^{-1}			

Table 2.2

Neutron Density:

The neutron density is used to calculate the power produced by nuclear fission events. A few simplifications are however made. The neutron density is considered as homogenous in the fuel rods. In the original point kinetics model a factor $\Psi(r)$ is considered to split the neutron population into two parts a time and spatially dependent part:

$$n(t,r) = n(t)\Psi(r) \tag{1.10}$$

Here the factor $\Psi(r)$ is considered 1 and therefore not used. So the following equation describes the neutron density (n).

$$\frac{dn}{dt} = \frac{\rho_{reactivity} - \beta}{\Lambda_{gen}} n(t) + \sum_{K=1}^{6} \lambda_K C_K(t) \tag{1.11}$$

The first term has the important factor $\rho_{reactivity}$; if the reactivity decreases $\frac{dn}{dt}$ gets lower and the neutron density will either increase slower or decrease faster. Λ_{gen} Is the mean neutron generation time which is the average time from a neutron emission to a capture that results in fission. So this describes the average time until a neutron is absorbed and induces another fission event. Neutrons that don't create another fission event are not taken into account. The second term takes delayed neutrons into account.

Delayed Neutron precursor:

For the neutron precursors the same time independent spatial correction is used, resulting in the following equation

$$C_i(t,r) = C_i(t)\Psi(r) \tag{1.12}$$

The following differential equation describes a neutron precursor's evolution

$$\frac{dC_K}{dt} = \frac{\beta_K}{\Lambda_{gen}} n(t) - \lambda_K C_K \tag{1.13}$$

Reactivity:

To calculate the reactivity an approximation is used (Schlagenhaufer[iii]). This approximation only considers the moderator density, so it ignores the influence of the reactor core temperature.

$$\rho_{reactivity} = \frac{k-1}{k} \rightarrow k = \frac{1}{1-\rho_{reactivity}} \tag{1.14}$$

$$\langle \alpha \rangle = \sum_{n_{in}}^{n_{out}} \frac{\alpha}{n_{out} - n_{in}} \tag{1.15}$$

$$\frac{d\rho_{reactivity}}{d\langle \alpha \rangle} = -14.24 * 10^{-6} * \langle \alpha \rangle + 0.04236 \tag{1.16}$$

Power:

There is a time delay between the moment of fission (the power release in the fuel) and the moment when the fluid is exposed to the resulting heat flux at the outer layer of the rod. This delay is mainly determined by the conductivity of uranium dioxide and the diameter of the rod. The delay is modeled by a first order differential equation:

$$\tau \frac{dq''}{dt} + q'' = w_f \Sigma_f \nu_n P n(t) \tag{1.17}$$

The value τ=0.5 s was used, this value was obtained by Kok en van der Hagen[iv]

Average

$$q''_{local} = \frac{q''}{n_{out} - n_{in}} \tag{1.18}$$

Steady State equations

The steady state equations are used to calculate the first steady state solution. The stability analysis is done by applying perturbation to the steady state solution and then linearizing the result. In the steady state equations the time derivatives are set to zero. For clarity the steady state variables get a bar in the notation: e.g. $\bar{x}$

Balance equations

Mass equation:

$$\frac{d\alpha_i}{dt} + \frac{G_i - G_{i-1}}{\Delta z} = 0 \rightarrow \tag{1.19}$$

Steady state

$$\bar{G}_i = \bar{G}_{i-1} \tag{1.20}$$

Momentum equation

$$\frac{\partial G_i}{\partial t} + \frac{1}{\Delta z}\left(\frac{G_i^2}{\alpha_i} - \frac{G_{i-1}^2}{\alpha_{i-1}}\right) + \frac{p_i - p_{i-1}}{\Delta z} = -g\rho_i \sin(\theta_i) - \frac{1}{2}\frac{G_i^2}{\alpha_i}\left[\frac{f_i}{D_H} + \frac{K_i}{\Delta z}\right] \rightarrow \tag{1.21}$$

Steady state

$$\frac{\bar{G}^2}{\Delta z}\left(\frac{1}{\bar{\alpha}_i} - \frac{1}{\bar{\alpha}_{i-1}}\right) + \frac{\bar{p}_i - \bar{p}_{i-1}}{\Delta z} = -g\bar{\alpha}_i \sin(\theta_i) - \frac{1}{2}\frac{\bar{G}^2}{\bar{\alpha}_i}\left[\frac{f_i}{D_H} + \frac{K_i}{\Delta z}\right] \rightarrow \tag{1.22}$$

$$\bar{p}_i = \bar{G}^2\left(\frac{1}{\bar{\alpha}_{i-1}} - \frac{1}{\bar{\alpha}_i}\right) - \Delta z\left(g\bar{\alpha}_i \sin(\theta_i) + \frac{1}{2}\frac{\bar{G}^2}{\bar{\alpha}_i}\left[\frac{f_i}{D_H} + \frac{K_i}{\Delta z}\right]\right) + \bar{p}_{i-1} \tag{1.23}$$

Energy equation:

$$\frac{d\alpha_i h_i}{dt} + \frac{G_i h_i - G_{i-1} h_{i-1}}{\Delta z} = q''_{local}\frac{P}{A} \rightarrow \tag{1.24}$$

Steady state

$$\frac{\bar{G}_i \bar{h}_i - \bar{G}_{i-1}\bar{h}_{i-1}}{\Delta z} = \bar{q}''_{local}\frac{P}{A} \rightarrow \tag{1.25}$$

$$\bar{h}_i = \frac{\Delta z}{\bar{G}}\left\langle \bar{q}''_{local} \right\rangle \frac{P}{A} + \bar{h}_{i-1} \tag{1.26}$$

Point Kinetics

Power:

$$\tau\frac{dq''}{dt} + q'' = w_f \Sigma_f v_n P n(t) \rightarrow \tag{1.27}$$

$$\bar{q}'' = w_f \Sigma_f v_n P \bar{n} \tag{1.28}$$

$$\bar{n} = \frac{1}{w_f \Sigma_f v_n P}\bar{q}'' \tag{1.29}$$

Delayed Neutronic Precursors:

$$\frac{dC_K(t)}{dt} = \frac{\beta_K}{\Lambda_{gen}} n(t) - \lambda_K C_K(t) \rightarrow \tag{1.30}$$

Steady state:

$$\bar{n} = \frac{\Lambda_{gen}\lambda_K}{\beta_K}\bar{C}_K \tag{1.31}$$

$$\bar{C}_K = \frac{\beta_K}{\Lambda_{gen}\lambda_K}\bar{n} \tag{1.32}$$

Neutron Density:

$$\frac{dn}{dt} = \frac{\rho_{reactivity} - \beta}{\Lambda_{gen}} n(t) + \sum_{K=1}^{6} \lambda_K C_K(t) \rightarrow \tag{1.33}$$

Steady state:

$$\bar{n} = \frac{\Lambda_{gen}}{\beta - \bar{\rho}_{reactivity}} \sum_{K=1}^{6} \lambda_K \bar{C}_K = \frac{\Lambda_{gen}\lambda_K}{\beta_K}\bar{C}_K \rightarrow \tag{1.34}$$

$$\sum_{K=1}^{6} \lambda_K \bar{C}_K = \frac{\left(\beta - \bar{\rho}_{reactivity}\right)\lambda_K}{\beta_K}\bar{C}_K \rightarrow \tag{1.35}$$

$$\sum_{K=1}^{6} \lambda_K \frac{\beta_K}{\Lambda_{gen}\lambda_K}\bar{n} = \frac{\left(\beta - \bar{\rho}_{reactivity}\right)\lambda_K}{\beta_K}\frac{\beta_K}{\Lambda_{gen}\lambda_K}\bar{n} \rightarrow \tag{1.36}$$

$$\sum_{K=1}^{6} \beta_K \bar{n} = \left(\beta - \bar{\rho}_{reactivity}\right)\bar{n} \rightarrow \tag{1.37}$$

$$\bar{\rho}_{reactivity} = 0 \tag{1.38}$$

Reactivity:

$$\frac{d\rho_{reactivity}}{d\langle\alpha\rangle} = -14.24 * 10^{-6} * \langle\bar{\alpha}\rangle + 0.04236 \tag{1.39}$$

In steady-state conditions the reactivity is 0; otherwise the power production would change.

Perturbed equations

After perturbing the equations, they are linearized resulting in a matrix form for the system of differential equations. Perturbation is done by adding a small disturbance to a steady state value:

$$x = \bar{x} + x' \tag{1.40}$$

The perturbed equations are linearized, neglecting higher order second order terms: $x'y'$. The time independent parts on the left and the right side of the equation are equal and can be removed. The density perturbation is approximated using a Taylor series expansion. The density is considered independent of pressure as there is only a small variation in the pressure over the system compared to 25 MPa.

Balance equations

Mass equation:

$$\frac{\partial \alpha_i}{\partial t} + \frac{G_i - G_{i-1}}{\Delta z} = 0 \rightarrow \tag{1.41}$$

Perturbed:

$$\left.\overline{\frac{d\alpha}{dh}}\right|_i \frac{dh'_i}{dt} = \frac{1}{\Delta z} G'_{i-1} - \frac{1}{\Delta z} G'_i \tag{1.42}$$

Momentum equation:

$$\frac{\partial G}{\partial t} + \frac{\partial}{\partial z}\left(\frac{G^2}{\alpha}\right) + \frac{\partial p}{\partial z} = -g\sin(\theta) - \frac{1}{2}\frac{G^2}{\alpha}\left[\frac{f}{D_H} + \sum_j K_j \delta\left(z - z_j\right)\right] \rightarrow \tag{1.43}$$

Perturbed:

$$\begin{aligned} \frac{dG'_i}{dt} = {} & \frac{2\bar{G}}{\Delta z \bar{\alpha}_{i-1}} G'_{i-1} - \left(\frac{2}{\Delta z} + \left[\frac{f_i}{D_H} + \frac{K_i}{\Delta z}\right]\right)\frac{\bar{G}}{\bar{\alpha}_i} G'_i - \frac{\bar{G}^2}{\Delta z \bar{\alpha}^2_{i-1}} \left.\overline{\frac{d\bar{\rho}}{dh}}\right|_{i-1} h'_{i-1} + \\ & \left(\frac{\bar{G}^2}{\Delta z \bar{\alpha}^2_i} - g\sin\theta_i + \frac{1}{2}\frac{\bar{G}^2}{\bar{\alpha}^2_i}\left[\frac{f_i}{D_H} + \frac{K_i}{\Delta z}\right]\right)\left.\overline{\frac{d\alpha}{dh}}\right|_i h'_i + \frac{1}{\Delta z} p'_{i-1} - \frac{1}{\Delta z} p'_i \end{aligned} \tag{1.44}$$

Energy equation:

$$\frac{d\alpha_i h_i}{dt} + \frac{G_i h_i - G_{i-1} h_{i-1}}{\Delta z} = q''_{local} \frac{P}{A} \rightarrow \tag{1.45}$$

Perturbed:

$$\frac{d\left(\bar{\alpha}_i h'_i + \bar{\alpha}'_i \bar{h}_i\right)}{dt} + \frac{G'_i \bar{h}_i + \bar{G}_i h'_i + -G'_{i-1} \bar{h}_{i-1} - \bar{G}_{i-1} h'_{i-1}}{\Delta z} = q'''_{local} \frac{P}{A} \rightarrow \tag{1.46}$$

$$\left(\bar{\alpha}_i + h_i \left.\overline{\frac{d\alpha}{dh}}\right|_i\right)\frac{dh'_i}{dt} = \frac{\bar{h}_{i-1}}{\Delta z} G'_{i-1} - \frac{\bar{h}_i}{\Delta z} G'_i + \frac{\bar{G}}{\Delta z} h'_{i-1} - \frac{\bar{G}}{\Delta z} h'_i + q'''_{local} \frac{P}{A} \tag{1.47}$$

Point Kinetics

Delayed neutronic precursors:

$$\frac{dC_K(t)}{dt} = \frac{\beta_K}{\Lambda_{gen}} n(t) - \lambda_K C_K(t) \tag{1.48}$$

Perturbed:

$$\frac{dC'_K}{dt} = \frac{\beta_K}{\Lambda_{gen}} n' - \lambda_K C'_K \tag{1.49}$$

Power:

$$\tau \frac{dq''}{dt} + q'' = w_f \Sigma_f v_n P n(t) \tag{1.50}$$

$$\tau \frac{d(q'')'}{dt} + (q'')' = w_f \Sigma_f v_n P n' \tag{1.51}$$

Reactivity:

$$\rho'_{reactivity} = \left(-14.24 * 10^{-6} * \langle \bar{\alpha} \rangle + 0.04236\right) \langle \alpha' \rangle \tag{1.52}$$

Neutron Density:

$$\frac{dn}{dt} = \frac{\rho_{reactivity} - \beta}{\Lambda_{gen}} n(t) + \sum_{K=1}^{6} \lambda_K C_K(t) \tag{1.53}$$

Perturbed:

$$\frac{dn'}{dt} = \frac{\left(-14.24 * 10^{-6} * \langle \bar{\alpha} \rangle + 0.04236\right) \langle \alpha' \rangle}{\Lambda_{gen}} \bar{n} + \frac{\bar{\rho}_{reactivity} - \beta}{\Lambda_{gen}} n' + \sum_{K=1}^{6} \lambda_K C'_K(t) \tag{1.54}$$

3. Instabilities

Types of instabilities

There are several types of instabilities, a primary classification is that of static and dynamic instabilities.
Static instabilities can be explained with steady-state equations an example is the Ledinegg instability, whereby a 'flow excursion' appears. This is driven by the occurrence of a negative slope in the pressure – flow rate curve. This results in 2 possible solutions (mass flow rate) for the same pressure drop and as such, the system can suddenly jump from one to the other driven by a small perturbation.

Dynamic instabilities are described by the time dependent equations, and are being studied in this thesis. These instabilities are mainly driven by the different feedback mechanisms in the system. There are several dynamic instabilities like "Pressure Drop Oscillations", "Acoustic Instabilities" and "Density Wave Oscillations" (DWO). The DWO are the most dominant instabilities.

A DWO can be explained by Figure 3.1, assume that the inlet flow (bottom part of the diagram) is oscillating. This flow rate oscillation travels through the channel, and as the enthalpy increases (higher up the channel), and the velocity differences start to increase. This results in increasing changes in the flow friction. In the middle part of Figure 3.1 the pressure drop at five points is plotted.

The total channel pressure drop (top part of Figure 3.1) now is the integration over the entire channel. This will also act sinusoidal driven by the flow rate perturbation. If the total pressure drop has a 180^{o} shift compared with the inlet flow, i.e. if the inlet-flow increases then the total pressure decreases, then the oscillation is self-sustaining, and therefore the system unstable.

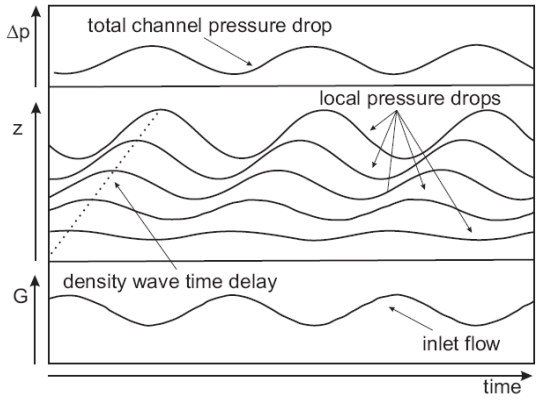

Figure 3.1 Illustration of density wave oscillation, figure adopted from Sanders[v]

It is important to note the difference between the conditions under which the instabilities can be modelled. The one is thermo-hydraulic, here the heat production is not influenced by the coolant flow or any other variable, the power is therefore constant. This was the case studied by G. Koren.

In this paper the coupled thermal-hydraulic and neutronic case is considered, here the power comes from nuclear fission. This fission is, amongst other factors, influenced by the enthalpy of the moderating fluid. In the case studied in this paper the coolant is also used as the moderating fluid so the power production is influenced by the coolant flow and the coolant flow influences the power production.

The dynamic instabilities are being calculated with differential equations, with solutions of the following form:

$$x = Ae^{\alpha t}e^{i(b+\beta t)} \tag{1.55}$$

It can easily be seen that if α is positive the function will diverge, while it will converge if α is negative. In discovering whether an initial state is stable or instable one can look at all possible eigenvalues belonging to the solutions (an eigenvalue has the form EV= $\alpha + i\beta$)looking for the highest value of α. If this is lower than zero the system is stable, otherwise it is unstable.

Dimensionless numbers

To allow for an easy comparison between different systems dimensionless numbers are introduced. In this paper the following ones are used.

$$N_{sub} \equiv \frac{h_{pc} - h_{in}}{h_{pc}} \tag{1.56}$$

$$N_{dh} \equiv \frac{q'}{GAh_{pc}} \tag{1.57}$$

h_{pc} is here the pseudo-critical enthalpy, h_{in} is the initial enthalpy of the water. As such, N_{sub} is constrained to values smaller than 1.

Neutral Stability Boundary

The Neutral Stability Boundary is an important concept in describing the flow behaviour of a SCWR. It is expressed in the dimensionless numbers N_{sub} and N_{dh} . It separates the stable region from the unstable region. The eigenvalue will be 0 on this boundary. For low values of N_{dh} the system will be stable, for high values the sytem will become unstable because of the higher power production. In between however there might be more Neutral Stability Points for one value of N_{sub}.

Analysis

Findnsb

The NSB is being calculated with the function *findnsb,* it works on the assumption that there is only one Neutral Stability Point for a single value of N_{sub}. In Figure 3.2 the method to determine the NSB is graphically represented. For each value of N_{sub} the highest eigenvalue of the solution of the matrix differential equation is calculated, if the eigenvalue is lower than zero a higher value for the power is

used, to calculate a new mass flux (G) and indirectly the new value of N_{dh}. If the highest eigenvalue is higher than zero a lower value of the power is used. This process is repeated until the border is first crossed or until the values of N_{dh} get to high to have physical meaning.

If the boundary is crossed, the process is repeated several times, until the highest eigenvalue approaches zero within a tolerance of 0.001. A Pegasus iteration method is used to achieve a faster convergence.

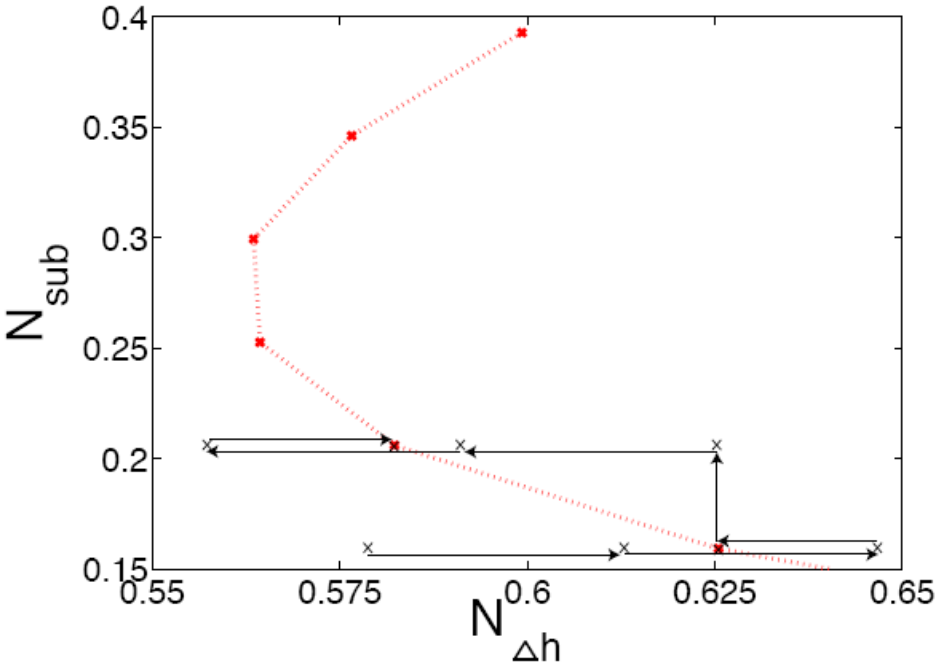

Figure 3.2Method used to find the NSB, figure adopted from Sanders[v]

4. Results

Ambrosini setup

In this study we consider the setup presented by ambrosini & Sharabi[vii]. The system is shown below, and the geometric parameters are listed in the Table 4.1. It consists of a tube with vertical upwards flowing supercritical fluid in between 2 reservoirs. As such, the pressure drop over the tube is imposed to 140 kPa.

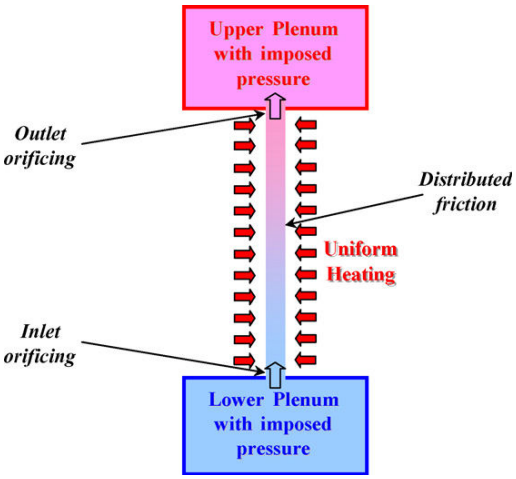

Basic setup

Unless otherwise specified the parameters used correspond to those in Table 4.1

Part	Value
channel length	4.2672 m
coolant ow area	5,49 *10^{-5} m^2
heated perimeter	32.04*10^{-3} m
system pressure	25*10^{6} Pa
inlet orifice pressure loss coefficient	27
outlet orifice pressure loss coefficient	0.75
Constant friction factor	0.0352
Hydraulic diameter	3.4*10^{-3} m

Table 4.1 parameters setup ambrosini

Steady state Benchmark

For the steady state case, there is no influence of the point kinetic model. A constant uniform power is assumed, which results in a spatially dependent pressure, enthalpy, velocity and density. The mass-flow rate is independent of time.

In order to match the results of Ambrosini (as inlet and outlet friction values and lengths were unknown), G. Koren used a pressure-height graph of Ambrosini to determine these values. After benchmarking the following result was obtained (Figure 4.1). A resolution of 11.2 cells per meter, a pressure drop of 0.139 MPa and an inlet-temperature of 280^{o}C was used. The resulting length of the valves is 0.05 m, and the inlet and outlet friction constants are 27 and 0.75 respectively.

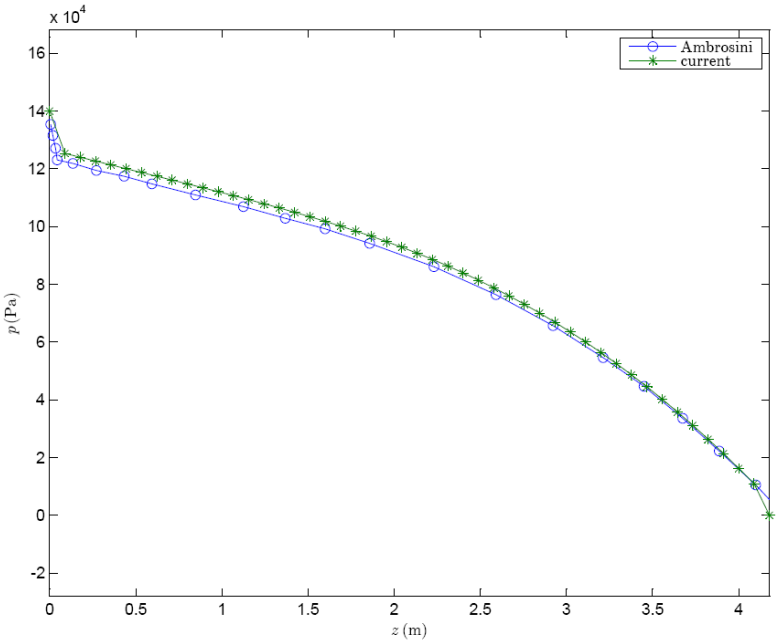

Figure 4.1 Comparing plot of pressure as a function of axial-distance between the current code and the simulation of Ambrosini. Figure adopted from G. Koren[vi].

To validate this result both the density and the velocity profile of the coolant were compared, see Figure 4.2.

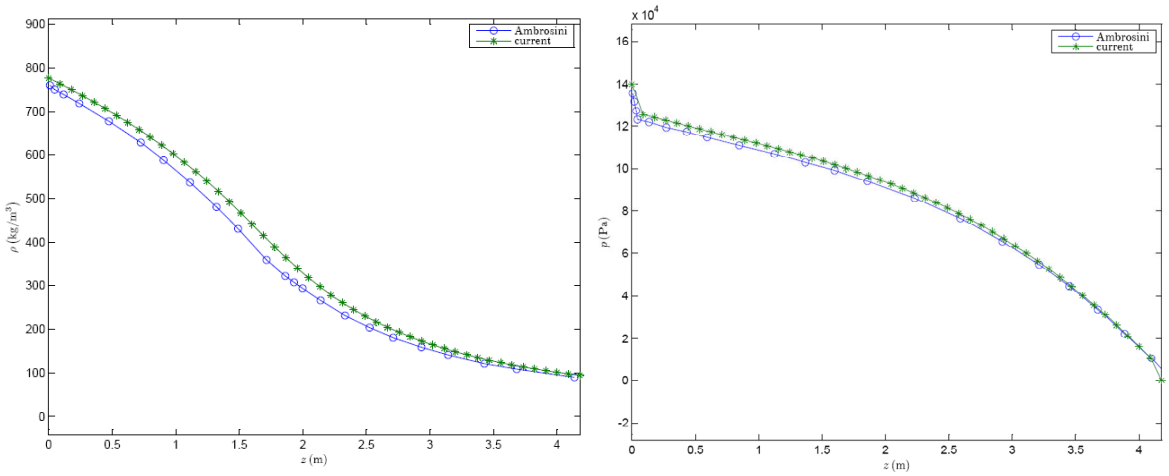

Figure 4.2 Comparing plots between the current code and the Results of Ambrosini, Left: Density versus axial height, right Pressure versus axial height, figure adopted from G. Koren[vi].

No neutronic feedback

Resolution dependence

The resolution (number of discretisations per meter) has a large influence on the calculation time: the smaller the grid the faster the simulations run. A resolution that is too low however gives wrong answers, for a resolution of 60 (m^{-1}) the solution seems to be optimal and there is little change for higher values, as indicated in Figure 4.3

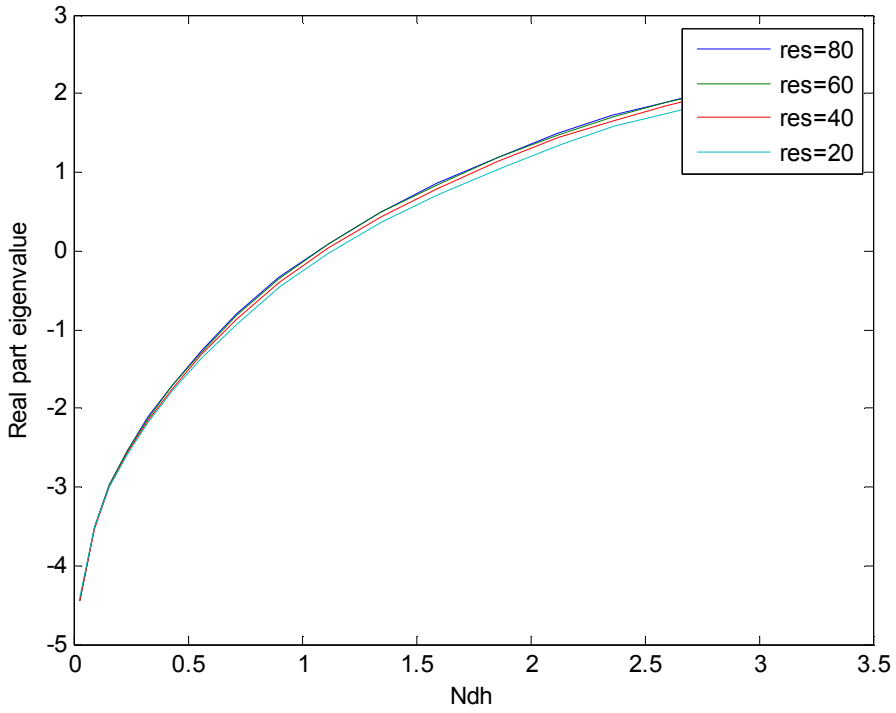

Figure 4.3: resolution dependence of eigscan, no neutronics, Nsub=0.3

Stability

The results for stability match the results obtained by ambrosini & Sharabi[vii]: increasing the friction at the inlet shifts, the stability line to higher values of Ndh. So the system becomes more stable consistent with DWOs.

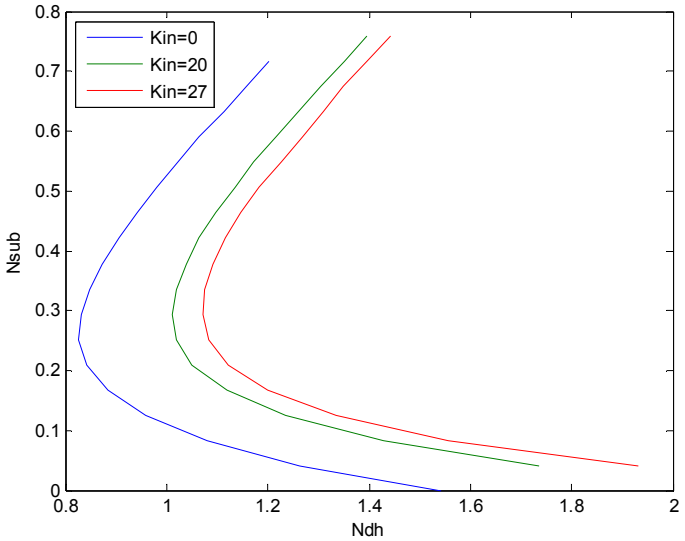

Figure 4.4 Influence of inlet friction on the stability, resolution-60.

The influence of the outlet friction is also consistent with previous studies: increasing its value makes the system less stable. This is shown in Fig. 4.5. The same can be said for raising the mean friction value in the tube, as shown in Fig. 4.6.

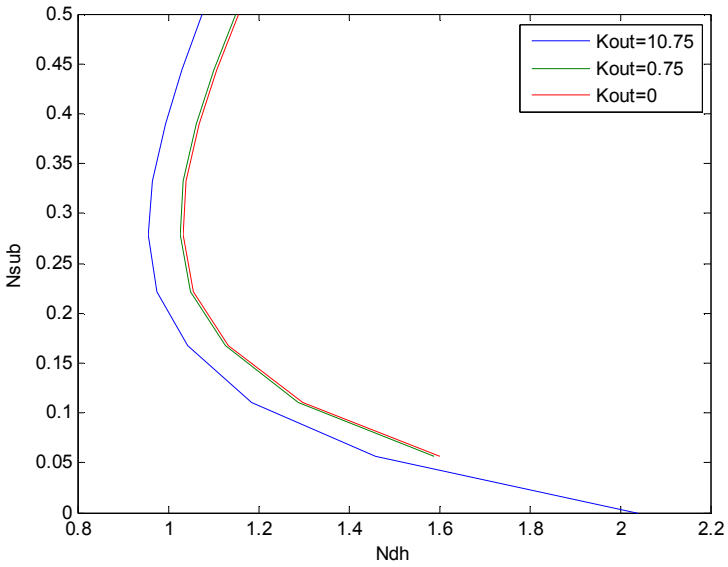

Figure 4.5 Influence of outlet friction on the stability, resolution=60.

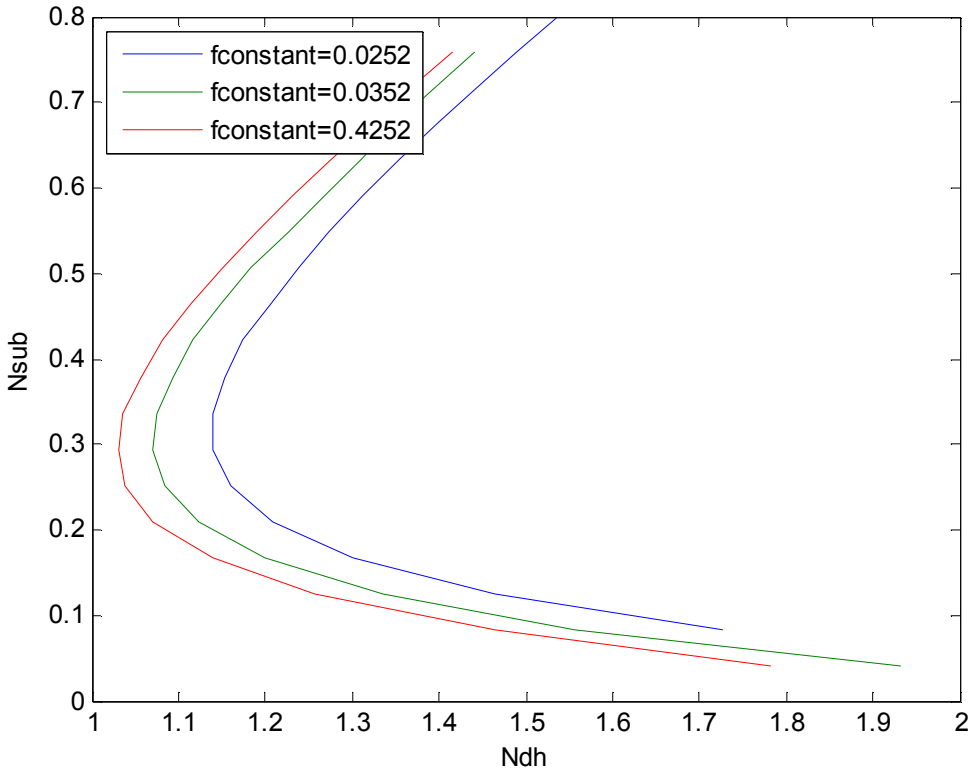

Figure 4.6: Influence of friction in the core on the stability, resolution=60.

Type of instability

The expected types of instabilities are DWO's. The average frequency of the numerically determined instabilities is 0.6 Hz (through the imaginary part of the eigenvalues), which fits in the expected range of 0.1 to 1 HZ (Gomez[viii]).

If you study a single core, the influence of friction can be explained by there contribution to the total pressure loss. An increase in friction causes an increase in pressure-drop, if is this increase is at a position in the core where the local pressure-drop oscillates in phase with the mass-flow, than it will make the flow more stable. An increase in friction at the entrance of the core will therefore always increase the stability. This corresponds to the results obtained as in Figure 4.4.

If the local pressure-drop at the outlet is out-of-phase with the mass-flow than an increase in outlet-friction will make the system more unstable.

The friction in the core is modelled as a constant factor, though it influences the local pressure-drops in the entire core its main influence on the stability lies in the fact that it changes the total mass-flow, and thereby the frequency at which it oscillates.

with point kinetic model

Resolution dependence

A first major difference that was found after implementation of the point kinetic model is that the resolution dependence of the model is much higher than without these equations. Figure 4.7 shows the dependence of the real part of the eigenvalue for varying grid sizes. This shows that at least a resolution of 80 cells per meter is required, but that there still are small shifts at higher values.

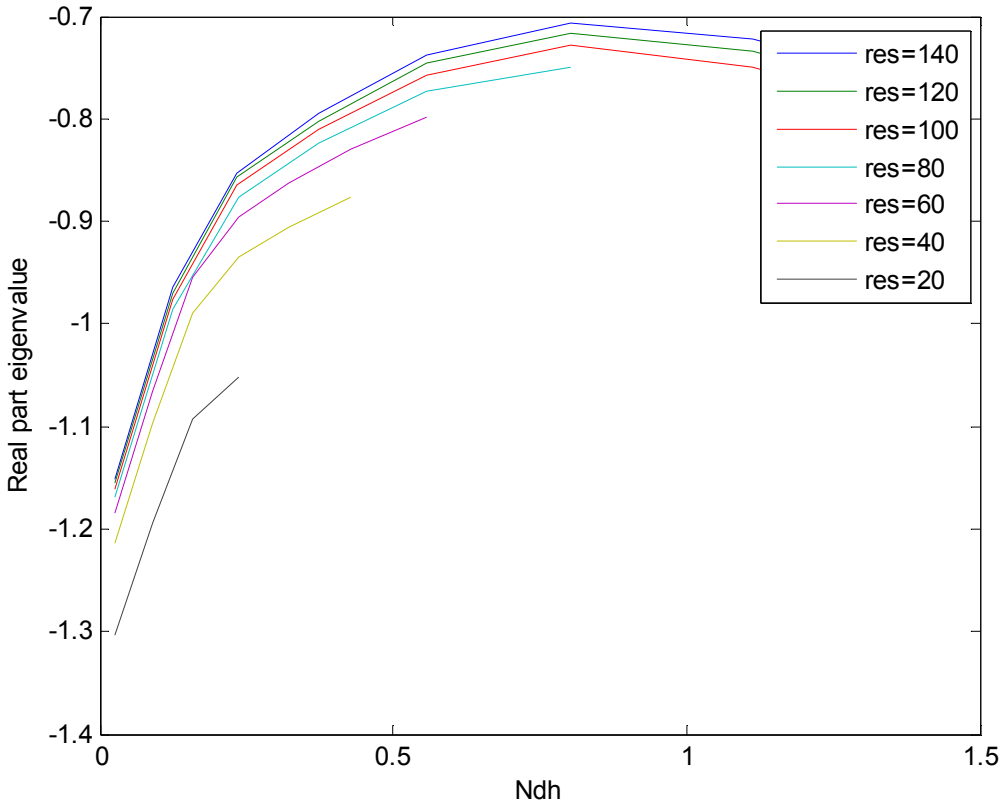

Figure 4.7: resolution dependence of eigscan

The eigenvalue solutions that are computed contain several unphysical ones, some of which have no imaginary part and therefore do not represent an oscillation, others have an infinite value. These latter are caused by the singular nature of the matrix. These solutions are removed from the list and not taken into consideration. As such, it is clear that for the simulations with point kinetics a higher resolution is required. This corresponds with the higher frequencies that are found for the dominant eigenvalues, the average frequency with point kinetics is about 1.5 Hz whereas without the average frequency is 0.6 Hz.

Another important difference between the two matrix models is the eigenvectors corresponding to the eigenvalues. For the case without point kinetics, the physical eigenvalues are linked to the mass

flux (Figure 4.8); the other eigenvalues are “infinite”. If the point kinetic model is implemented however the solutions of the differential equation correspond to the enthalpy.

This can be expected, as in the new equations there is an extra term in the energy equation, the energy equations are now directly related to the density, mass flow and power production.

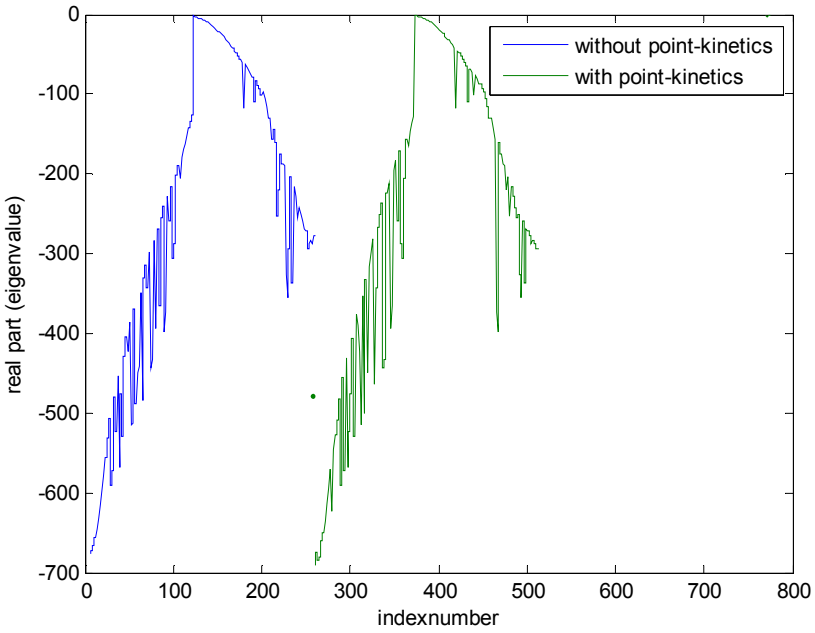

Figure 4.8: Eigenvalues, for both the situation with and without point-kinetics, corresponding to the eigscan at Ndh=0.5 and Nsub =0.2. The first 257 points correspond to the mass -flow, points 258 up to 314 correspond to the enthalpy of the coolant and the last 257 point correspond to the pressure.

A stranger phenomenon is that when the stability is being studied at higher values of Ndh, the former regular NSB-line start to oscillate in an unpredictable way. Sometimes this happens when the physical properties retrieved from the NIST data reach their boundaries, but not always. This problem can be controlled by increasing the resolution, this suggests that the values that don’t follow the smooth line can be regarded as unphysical or incorrect.

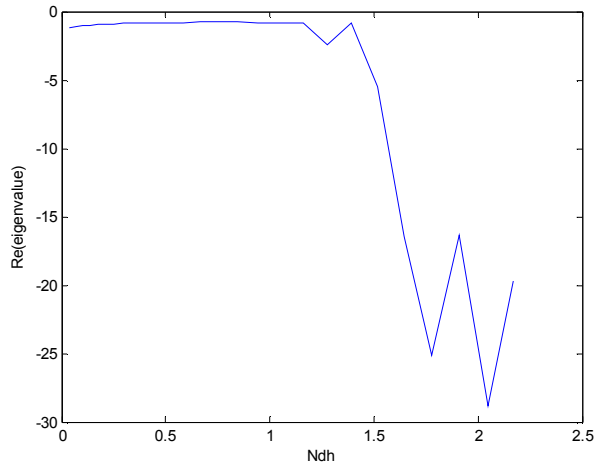

Figure 4.9:eigscan for model with Point Kinetics, above Ndh=1.2 the line is no longer smooth

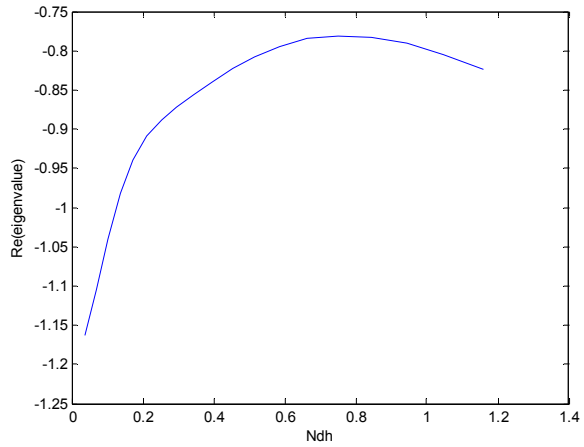

Figure 4.10eigscan for model with Point Kinetics, Ndh max=1.2

Another indication that “strange” things are happening is that the eigenvalues no longer correspond to the enthalpy but also to the pressure (Figure 4.11).

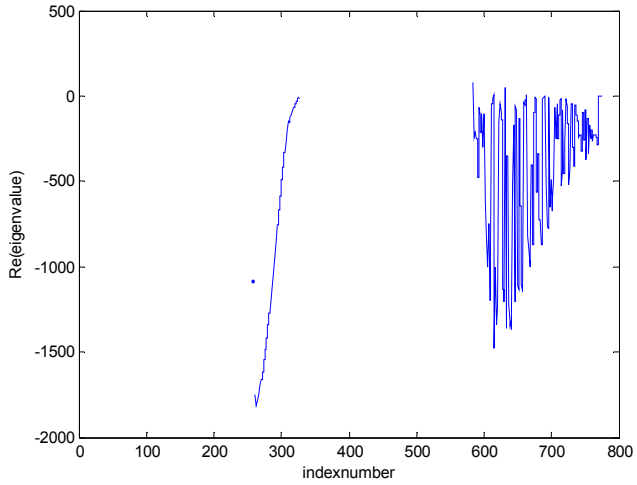

Figure 4.11: Eigenvalues corresponding to Ndh=0.917, Nsub =0.2 with point kinetics.

Stability

In the coupled thermohydraulic-neutronic calculations no instabilities found that have a physical meaning. This would suggest that the system with point kinetics is very stable.

It is however possible to look at the effects of the different frictions, by looking at the eigscan. Here the highest real part of an eigenvalue (with an imaginary part) is being plotted at different Ndh, and a constant Nsub.

The higher the inlet friction the more unstable the system seems to become, this can't be said with certainty for the neutral stability boundary is never reached (note that there is no instability, just that the real part of the eigenvalues gets closer to 0 with increasing inlet friction).
If the system really does get more unstable this would be in contradiction with the expectations because an increase in inlet friction has an expected result of in increase in stability.

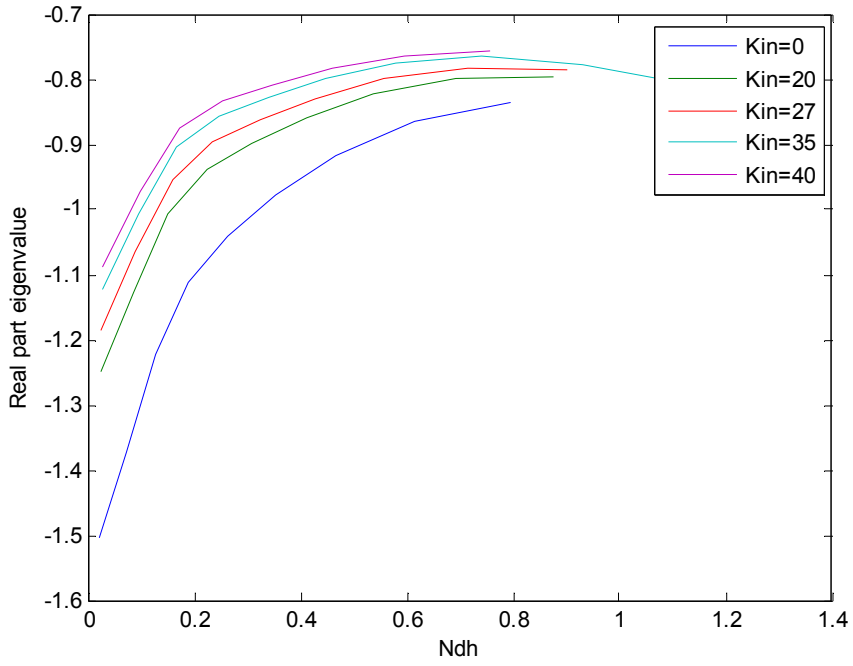

Figure 4.12 Eigscan with point kinetics, variation in inlet friction, Resolution=60, Nsub=0.2.

Friction in the core

The friction in the core has the same effect as the inlet friction, the friction is modelled as a constant.

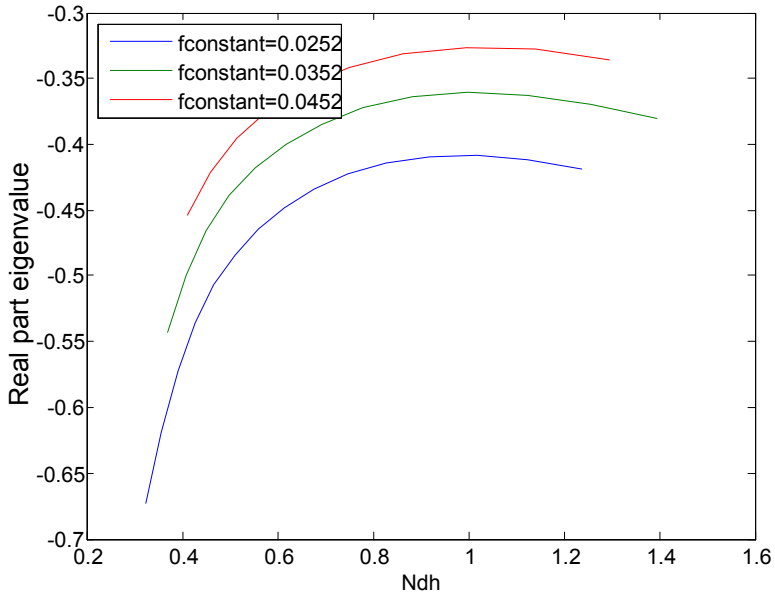

Figure 4.13: eigscan with point kinetics, variation fconstant. Nsub =0.4

Friction in the outlet

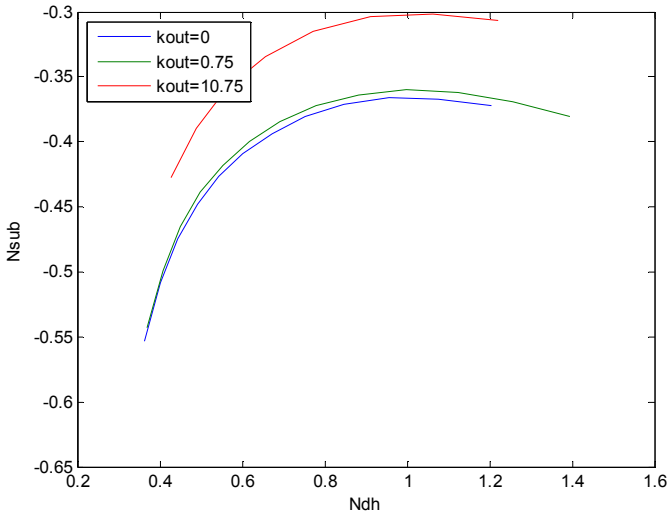

Figure 4.14:eigscan with point kinetics, variation outlet friction (Nsub=0.4)

As mentioned in before in this chapter, the unstable region can't be reached, it can however be studied what happens with the most unstable solution if K_{out} is changed. The graph clearly shows that an increase in K_{out}. This might suggest a more unstable situation; this can't be said with certainty for the neutral stability boundary is never reached.

Influence Point-Kinetic Variables

Changing variables has no effect, putting a factor (>0) in front the neutron generation time, or the time delay doesn't influence the result of eigscan i.e. the highest real eigenvalue remains the same.

Mean neutron generation time

The mean neutron generation time showed not to have any influence on the stability; the physical meaningful results were unchanged by this variable.
The point where the results start to become physically meaningless changes however, the higher the mean neutron generation time the longer (for the higher Ndh) meaningful result are obtained. It is unlikely that the results after the point where the eigscan "jumps" is physically meaningful, because this point can be shifted to a higher value of Ndh with a higher resolution.

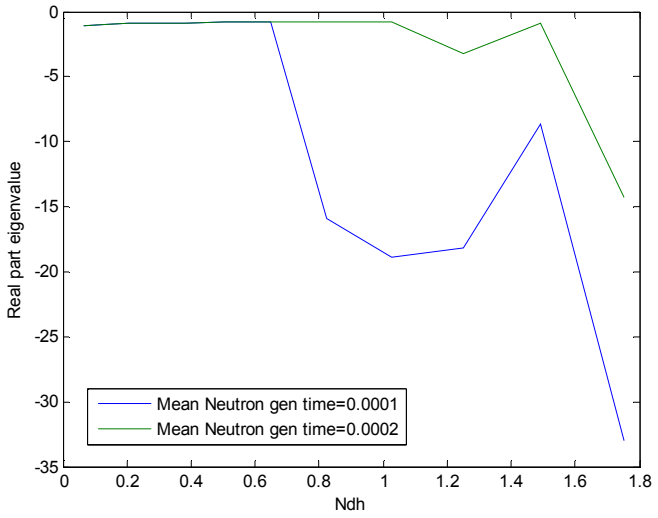

Figure 4.15, eigscan with point kinetics, Nsub=0.2, resolution=60.

The effect on the eigenvalues is more clear, the higher the mean neuron generation time, the more the plot of the real part vs the imaginary part of all eigenvalues represents an ellipse.

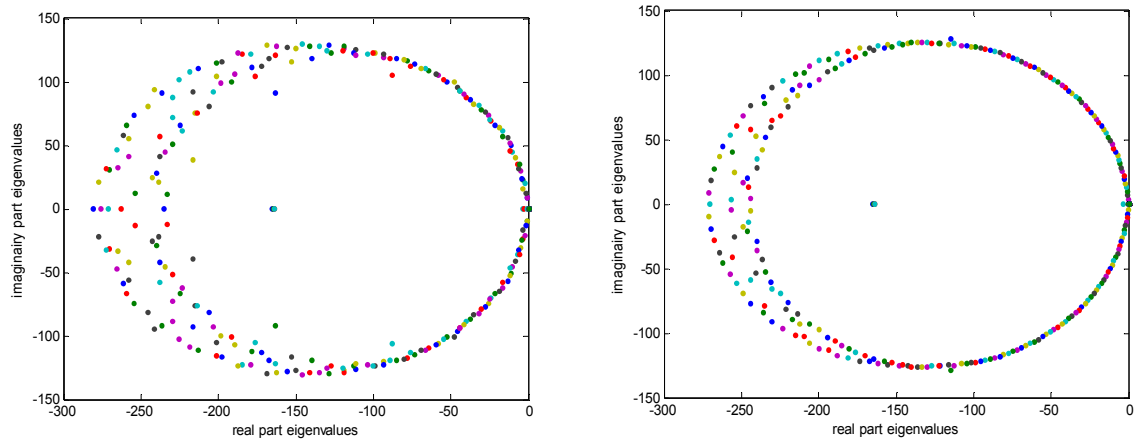

Figure 4.16 the real part of the eigenvalues plotted against the imaginary part, Nsub=0.5, Ndh=0.3. Left: mean neutron generationtime=0.0001 s, right: 0.001 s.

Time delay

The constant τ, used to model the time delay between energy production in the core to the point it reaches the coolant at the cladding, also has no influence on the eigscan

The coupling between the power production and the neutron density seems not to work however, for changing τ from 4 to 2 changes one eigenvalues from -0.25 to -.5. The power was described by equation (1.17) $\tau \frac{dq''}{dt} + q'' = w_f \Sigma_f v_n Pn(t)$ putting a factor in front of the right part of this equation also has no influence. A possible explanation might be found in the one “Not a Number” that appears as an eigenvalue.

Reactivity

The reactivity is modelled by equation (1.16) $\frac{d\rho_{reactivity}}{d\langle\alpha\rangle} = -14.24 * 10^{-6} * \langle\bar{\alpha}\rangle + 0.04236$

The steadystate density ($\langle\bar{\alpha}\rangle$) is independent of the neutronics, so $\frac{d\rho_{reactivity}}{d\langle\alpha\rangle}$ can be seen as a constant, the influence of this factor is opposite to the mean neutron generation time, If the value is lower there can be obtained physical meaningful results for higher Ndh.

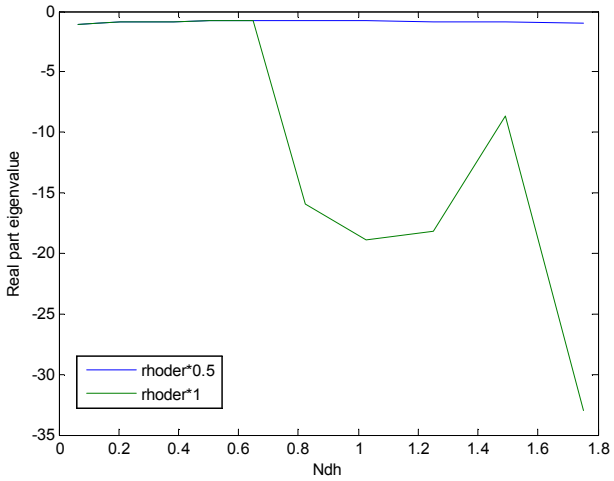

Figure 4.17 eigscan with point kinetics, Nsub=0.2, resolution=60. rhoder= $\frac{d\rho_{reactivity}}{d\langle\alpha\rangle}$

With lower values of this factor the plot of the real part of all eigenvalues vs. the imaginary part approaches an ellipse (see Figure 4.18).

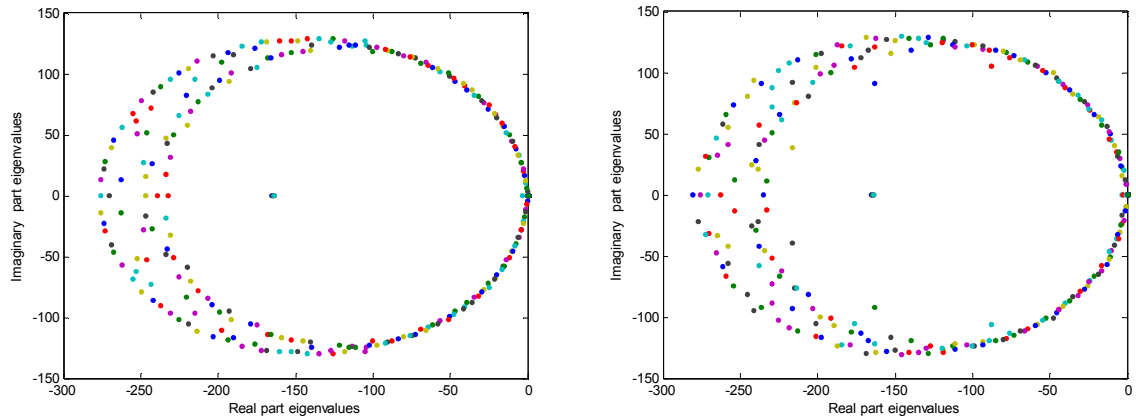

Figure 4.18 the real part of the eigenvalues plotted against the imaginary part, Nsub=0.5, Ndh=0.3. On the left $\frac{d\rho_{reactivity}}{d\langle\alpha\rangle}$ is multiplied with 0.5 on the right it is multiplied with 1.

5. Conclusions and recommendations

Conclusions

Unfortunately there is not much material to compare the findings of the Coupled Thermal-Hydraulic /Neutronic instabilities.
Gomez[viii] however suggests that there is a Neutral Stability Boundary. This is a diametrical different result from the results obtained in this study, and suggests a flaw in the code. Also the lack of coupling between the power and the neutron density suggests a flaw in the code.

If the results are however correct this would be very encouraging, it would mean that, at least in a setup with imposed pressure and inlet enthalpy, an unstable situation will never occur. And furthermore, that the mean-neutron-generation-time and the time-delay don't influence the stability of the flow significantly.

Error

The lack of coupling between power and neutron density, and the difference with the results of Gomez[viii] give reason to doubt the result, a review of the code is therefore useful. An alternative way to calculate the eigenvalues also might be considered.

Setup

The setup used is a simplified system with a constant pressure difference over the riser, a more realistic setup can be studied. For example a setup which takes the flow between the outlet and the inlet of the riser in account.
Also a loop with natural convection (no pump but circulation due to density differences under influence of gravity) would be very interesting.

Heat transfer

In the model a constant time delay between the heat production in the rods till the transfer from the cladding to the coolant is assumed. If the heat transfer is calculated with the thermal conductivity of the fuel and the cladding than the temperature in the fuel can be known. This would also allow to take the influence of the core temperature on the reactivity in account.

6. Bibliography

[i] US DOE Nuclear Energy Research Advisory Committee, A technology road map for Generation IV nuclear energy systems, Technical report, Generation IV International Forum, (2002).

[ii] J. Duderstadt and L. Hamilton, Nuclear Reactors Analysis, Cambridge University Press, 1976.

[iii] M. Schlagenhaufer Reactivity Control Mechanisms for a HPLWR Fuel Assembly,

[iv] H. V. KOK and T. H. J. J. VAN DER HAGEN, "Design of a Simulated Void-Reactivity Feedback in a Boiling Water Reactor Loop," Nucl. Technol., 128, 1 (1999).

[v] M.B. Sanders. Thermo-hydraulic stability analysis of the high performance light water reactor and a scaled experimental facility. Master's thesis, TU Delft, Faculty of Applied Sciences, Delft, The Netherlands, 2009.

[vi] G. Koren. Linear Stability Analysis of a Supercritical Water Loop, driven by Natural convection.

[vii] W. Ambrosini and M. Sharabi. Dimensionless parameters in stability analysis of heated channels with uids at supercritical pressures. Nuclear Engineering and Design, 238(2008) 1917 -1929.

[viii] T. Gomez. Stability Analysis of the High Performance Light Water reactor. PhD thesis, Forchungszenttum Karlsruhe, Karlsruhe, Germany, 2008